Computer-aided optimization in additive manufacturing: Processing parameters and 3D scaffold reconstruction

Cite as: AIP Conference Proceedings **2116**, 230005 (2019); https://doi.org/10.1063/1.5114231
Published Online: 24 July 2019

Nuno Alves, Miguel Belbut Gaspar, and Paula Pascoal-Faria

Computer-Aided Optimization in Additive Manufacturing: Processing Parameters and 3D Scaffold Reconstruction

Nuno Alves[1,2, a)]; Miguel Belbut Gaspar[1, b)] and Paula Pascoal-Faria[1,2, c)]

[1]*Centre for Rapid and Sustainable Product Development, Mechanical Engineering Department of the School of Technology and Management, Polytechnic Institute of Leiria, Portugal*

[2]*Centre for Rapid and Sustainable Product Development, Mathematics Department of the School of Technology and Management, Polytechnic Institute of Leiria, Portugal*

[a)]Corresponding author: nuno.alves@iplreiria.pt
[b)]Miguel.belbut@iplreiria.pt
[c)]paula.faria@iplreiria.pt

Abstract. Scaffolds are implantable bio-absorbable systems capable of regenerating osteoporotic bone or other native tissues. Additive Manufacturing processes are used to produce scaffolds with customized external shape and predefined internal morphology, allowing some control over pore size and distribution. Despite significant advances in Additive Manufacturing processes, the experimental optimization of processing parameters is time-consuming and expensive usually generating biomaterials waste. Moreover, the manufacturing of such polymeric or hybrid scaffolds requires time-consuming human supervision procedures. Subsequently, measurements of the scaffold's architecture such as filament diameter, distance between two consecutive filaments, pore geometry and size, and total porosity are usually performed using computer tomography or microscopy, which also requires significant human and physical resources. This research work intends to overcome some aforementioned limitations through the development of a novel approach based on *in-situ* computer-aided optimization of the extrusion-based processing parameters.

INTRODUCTION

Osteoporosis (OP) is a disorder of unbalanced bone remodeling which occurs when bone resorption exceeds bone formation, resulting in low density bones with poor mechanical properties [1]. Patients with OP are at great risk of bone fracture after minimal trauma leading to high health care expenses and decreased life quality. Several groups worldwide are working on three-dimensional (3D) scaffold-based tissue engineering (TE) aiming the development of new therapies for treatment of bone (or other tissue) diseases [2, 3, 4, 5, 6, 7]. A key related work was reported by Atala [8] which specifies that one of the most important TE methodologies is the combination of 3D scaffolds with autologous cells to produce bioimplants capable of promoting tissue regeneration. These implantable and bio-absorbable 3D bio-constructs with customized external shape and predefined internal morphology, allowing some control over pore size and distribution, are typically produced using additive manufacturing (AM) technologies [4, 9, 10]. Here, we focus in the extrusion-based AM processes to produce bio-constructs for TE applications, where 3D scaffold design (geometry parameters), materials, and fabrication (processing parameters) play a key role.

Despite significant advances in extrusion-based AM processes, several restrictions still due to experimental optimization and time-consuming human supervision procedures. Thus, this research intends to overcome some of these limitations through the development of a novel *in-situ* computer-aided optimization (INCA) approach for extrusion-based AM processes, allowing better control over customized 3D scaffold architecture. The paper describes the INCA approach for extrusion-based processing parameters such as liquefier temperature (LT), deposition velocity (DV) and screw rotation velocity (SRV). 3D scaffold reconstruction is out of scope of this manuscript.

International Conference of Numerical Analysis and Applied Mathematics (ICNAAM 2018)
AIP Conf. Proc. 2116, 230005-1–230005-5; https://doi.org/10.1063/1.5114231
Published by AIP Publishing. 978-0-7354-1854-7/$30.00

MATERIALS AND METHODS

Sample Design and Manufacturing

Figure 1a shows a typical 3D scaffold design and the related physical scaffold (Fig. 1b) manufactured using the BIOMATE system (Fig.1c), a home-made extrusion-based AM system. FG, FD, FW, ST and LG denote the filament gap, filament distance, filament width, slice thickness and layer gap, respectively.

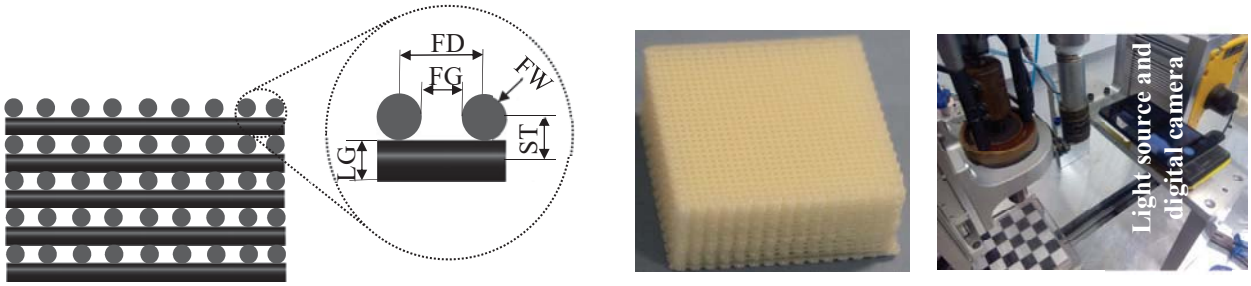

(a) (b) (c)

FIGURE 1. Cross-section of a typical 3D scaffold design (a), physical 3D scaffold (b), and the BIOMATE system (c).

To study optimal processing parameters (DV, SRV and LT) using the INCA approach, a simple two-layer scaffold was designed as illustrated in Fig. 2a. Two layers are the minimum required, since the first layer is not representative of the material behavior in the bulk of a manufactured multi-layer scaffold. Figure 2b illustrates the toolpaths for bottom and top layers (z -axis scaled 4x for clarity). Green and red markers indicate the start and stop of each layer. The DV used in the top layer varied from 200 to 900 mm/min (with increment of 50 mm/min) thus producing 15 filaments at 15 different DV using a nozzle diameter of 400 µm at constant LT of 80º C and SRV of 18 rpm. Six scaffold samples were fabricated using six different values of SRV: 18, 23, 28, 33, 38, and 43 rpm. In total, eighteen scaffold samples were produced using three nozzle diameters of 300, 400, and 500 µm and polycaprolactone (PCL) with an Mw = 50,000 Da (CAPA 6500). Thus, each printed filament width is a function of the scaffold geometry and processing parameters (eq. 1).

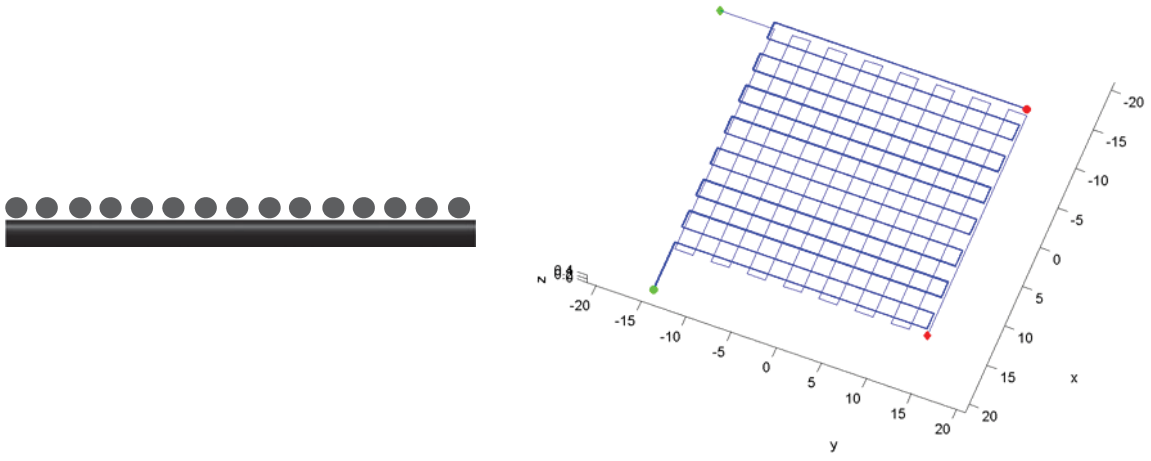

(a) (b)

FIGURE 2. Scaffold sample design (a), and bottom and top toolpaths (b) used for AM processing parameters optimization.

$$\mathrm{FW} = FW(FD, FG, ST, LG, DV, SRV, ND, M) \quad (1)$$

M is the type of material used to print the scaffold. Here, the main objective is to automatically optimize the printed filament width through the application of the INCA approach according to a specific nozzle diameter used.

Detection of Region of Interest and Filament Characterization

The image acquisition of the scaffold samples was performed using a digital camera with specifications described in Table 1.

TABLE 1. Digital camera specifications.

Resolution	Aperture	Sensor diagonal	Pixel size	Color depth	Exposure	Focal distance
13 MP	f/2.0	1/3"	1.12 µm	24 bit, sRGB	1/60 s	4 mm (eq. 27 mm)

The region of interest ROI (scaffold) and scale factor were automatically computed through the Algorithm 1.

ALGORITHM 1. Determination of the region of interest and scale factor

Objective:

Given 1 digital image of a two-layer scaffold sample, determine the threshold for separation of specular highlights, top and bottom filaments, and filament characterization.

Procedure:

1. Run Hough Transform on sub-sampled binary image of top filaments (detects lines parameterized by slope and distance to origin).
2. Determine a loose bounding box and approximate rotation.
3. Determine, accurately, the bounds and scale factor on the straightened and cropped full resolution gray scale image.
4. Perform the filament characterization (filament diameter) based on pixel count: compute the mean number of pixels in each sub-image of the binarized image

Figure 3a shows a digital image of a two-layer scaffold sample attached to the work platform of the BIOMATE system, including the identification of the bottom and top lines. Accurate computed ROI and filaments detection are shown in Figure 3b. Top line is the intensity profile of the binarized image and bottom is the intensity profile for the gray-scale image.

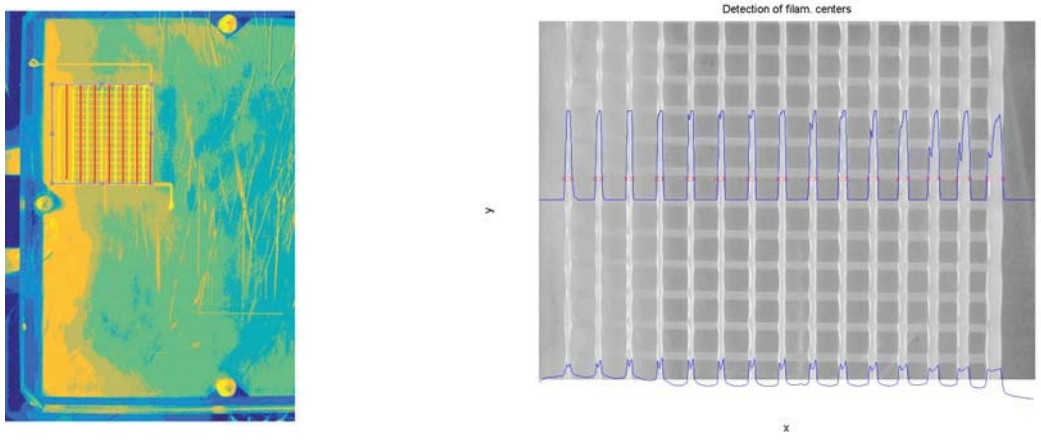

(a) (b)

FIGURE 3. Digital image of a two-layer scaffold attached to the work platform including the identification of bottom and top lines (a). Accurate filaments detection in the cropped gray-scale image (b).

RESULTS AND DISCUSSION

Suitable imaging processing techniques were used to *in-situ* automatically compute filament width as a function of AM extrusion-based processing parameters such as deposition velocity and screw rotation velocity at a constant liquefier temperature for three nozzle diameters using PCL. Figure 4 summarizes the values obtained for FW as a function of DV, SRV, LT = 80ºC, and a nozzle diameter of 400µm.

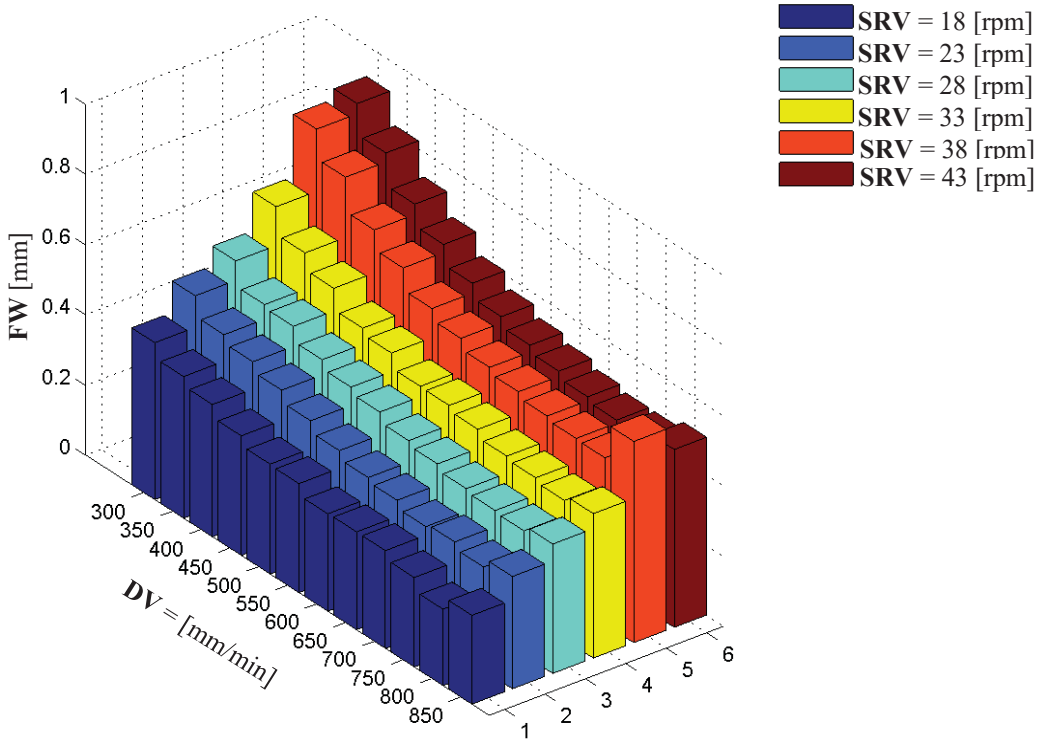

FIGURE 4. Filament width (FW) as a function of the processing parameters DV and SRV, at a constant liquefier temperature (LT = 80ºC) and a nozzle diameter of 400µm.

Results suggest a non-linear function to modulate FW as a function of DV and SRV. As expected, FW increases as DV decreases and SRV increases.

CONCLUSIONS

The *in-situ* computer-aided optimization (INCA) approach for extrusion-based AM processes is able to automatically determine the optimal values of DV and SRV, comparing FW values with nozzle diameter used to print 3D scaffolds. Current limitations such as human experimental processing parameters optimization and time-consuming human supervision procedures can be surpassed through the use of the INCA approach, allowing a better control over customized 3D scaffold architecture as well reducing the biopolymer waste.

ACKNOWLEDGMENTS

This work is supported by the Portuguese Foundation for Science and Technology (FCT) and Centro2020 through the Project references: UID/Multi/04044/2019; PAMI – ROTEIRO/0328/2013 (Nº 022158); MATIS (CENTRO-01-0145-FEDER-000014 – 3362) and BioMaTE - POCI-01-0145-FEDER-016800.

REFERENCES

1. L. Cruz, E. Assumpção, S. Andrade, D. Conrado, I. Kulkamp, S. Guterres and A. Pohlmann, European Journal of Pharmaceutical Sciences **40**, 441-447 (2010).
2. M. Arafat, C. Lam, A. Ekaputra, S. Wong, C. He, D. Hutmacher, X. Li and I. Gibson, Soft Matter. **7**, 8013-8022 (2011).
3. S. J. Hollister, Nature Materials **4**, 518–524 (2005).
4. P. Morouço, S. Biscaia, T. Viana, M. Franco, C. Malça, A. Mateus, C. Moura, F. Ferreira, G. Mitchell and N. Alves, BioMed Research International **2016**, 1-10 (2016).
5. P. Morouço, W. Lattanzi and N. Alves, Frontiers in Bioengineering and Biotechnology **5**, (1-3) (2017).
6. U. Jammalamadaka and K. Tappa, J Funct Biomater. **9**, 22-35 (2018).
7. L. Dong, S.Wang, X. Zhao, Y. Zhu and J. Yu, Scientific Reports **7**, 1-9 (2017).
8. A. Atala, Journal of Tissue Engineering and Regenerative Medicine **1**, 83-96 (2007).
9. M. Domingos, F. Chiellini, A. Gloria, L. Ambrosio, P. Bartolo, E. Chiellini, Rapid Prototyping Journal. **18**, 56-67 (2012).
10. L Francisco, C Moura, T Viana, D Ângelo, P Morouço and N Alves, Procedia Manufacturing **12**, 91-97 (2017)